



Provided by the author(s) and University of Galway in accordance with publisher policies. Please cite the published version when available.

Title	Volcanic sulphate and arctic dust plumes over the North Atlantic Ocean
Author(s)	Ovadnevaite, Jurgita; Ceburnis, Darius; Dupuy, Regis; Berresheim, Harald; O Dowd, Colin D.
Publication Date	2009
Publication Information	Ovadnevaite, J., Ceburnis, D., Plauskaite-Sukiene, K., Modini, R., Dupuy, R., Rimselyte, I., et al. (2009). Volcanic sulphate and arctic dust plumes over the North Atlantic Ocean. <i>Atmospheric Environment</i> , 43(32), 4968-4974.
Publisher	Elsevier
Link to publisher's version	http://dx.doi.org/10.1016/j.atmosenv.2009.07.007
Item record	http://hdl.handle.net/10379/721

Downloaded 2024-04-28T23:13:47Z

Some rights reserved. For more information, please see the item record link above.



1 Volcanic sulphate and Arctic dust plumes over the North Atlantic Ocean

2
3 J. Ovadnevaite^{1,2,*}, D. Ceburnis¹, K. Plauskaite-Sukiene², R. Modini³, R. Dupuy¹, I. Rimselyte²,
4 M. Ramonet⁴, K. Kvietkus², Z. Ristovski³, H. Berresheim¹ and C. D. O'Dowd¹

5
6 ¹ School of Physics and Centre for Climate and Air Pollution Studies, Environmental Change
7 Institute, National University of Ireland, Galway, Ireland

8 ² Institute of Physics, Savanoriu 231, LT-02300 Vilnius, Lithuania

9 ³ ILAQH, Queensland University of Technology, 2 George Street, Brisbane 4000 QLD, Australia

10 ⁴ Laboratoire des Sciences du Climat et de l'Environnement (LSCE), Gif sur Yvette, France

11 *Corresponding author: E-mail address: jurgita.ovadnevaite@nuigalway.ie, Tel.: +35391492496,
12 Fax. : +35391494584, Address: School of Physics and Centre for Climate and Air Pollution
13 Studies, Environmental Change Institute, National University of Ireland, Galway, Ireland

14
15 **Abstract.** High time resolution aerosol mass spectrometry measurements were conducted during
16 a field campaign at Mace Head Research Station, Ireland, in June 2007. Observations on one
17 particular day of the campaign clearly indicated advection of aerosol from volcanoes and desert
18 plains in Iceland which could be traced with NOAA Hysplit air mass back trajectories and
19 satellite images. In conjunction with this event, elevated levels of sulphate and light absorbing
20 particles were encountered at Mace Head. While sulphate concentration was continuously
21 increasing, nitrate levels remained low indicating no significant contribution from anthropogenic
22 pollutants. Sulphate concentration increased about $3.8 \mu\text{g}/\text{m}^3$ in comparison with the background
23 conditions. Corresponding sulphur flux from volcanic emissions was estimated to about 0.3
24 TgS/yr, suggesting that a large amount of sulphur released from Icelandic volcanoes may be

25 distributed over distances larger than 1000 km. Overall, our results corroborate that transport of
26 volcanogenic sulphate and dust particles can significantly change the chemical composition, size
27 distribution, and optical properties of aerosol over the North Atlantic Ocean and should be
28 considered accordingly by regional climate models.

29

30 *Key Words:* volcanic sulphate aerosol, Icelandic dust, particle acidity, aerosol properties

31

32 **1. Introduction**

33 Sulphuric acid and sulphate aerosols are essential precursors for cloud formation over the oceans
34 (Charlson et al., 1987). They act as a cloud condensation nuclei and affect the number of cloud
35 droplets increasing cloud albedo and may also lead to changes in precipitation (Textor et al.,
36 2004). Nss-sulphate over the oceans can originate from both natural and anthropogenic sources
37 and concentrations vary widely as a function of time and location (Savoie et al., 2002). Volcanic
38 emissions of SO₄ and its sulphur precursor gases can significantly contribute to the natural SO₄
39 budget, even at the quiescent stage (Berresheim and Jaeschke, 1983; Glasow et al., 2008).
40 According to Graf et al. (1997) the non-eruptive volcanic degassing of SO₂ and subsequent
41 sulphate formation is estimated to be responsible for 24% of the global annual direct radiative
42 forcing of sulphate aerosols. The annual SO₂ flux into the atmosphere from Icelandic volcanoes
43 is about 0.8-1.0 Tg/yr (Halmer et al., 2002) thus representing one of the largest atmospheric
44 sulphur sources in the North Atlantic region. These emissions may substantially contribute to
45 new particle formation over this region and modify the composition of air masses, for example,
46 of clean polar origin (O'Dowd and Smith, 1993).

47 Furthermore, Iceland has extensive arid regions, which are seldom reported in surveys, because
48 the climatic environment and the composition of the sand make these deserts unusual. The sand

49 originates largely from glacial margins, glacio-fluvial and volcanic deposits, and sedimentary
50 rocks (Arnalds et al., 2001). Strong winds can generate dust storms over these deserts, and dust
51 plumes may be transported over great distances impacting air quality in the British Isles and
52 continental Europe (NASA, 2008; Prospero et al., 2008). Although dust storms may at times be
53 relatively rare events, Prospero et al. (2008) pointed out that glaciers in Iceland have been
54 retreating in recent decades and that this trend is expected to continue with changing climate. It
55 is difficult to track the sulphate and dust plumes by composition analysis which is typically done
56 with off-line techniques in long-term monitoring programmes such as Global Atmosphere Watch
57 (GAW). Here we report real-time observations using a quadrupole aerosol mass spectrometer
58 (Q-AMS) at the Mace Head Atmospheric GAW Research Station, on the west coast of Ireland,
59 which enabled high time resolution measurements of size spectra and concentrations of organic
60 and inorganic species in the sampled particles. Together with other real time measurement
61 techniques operated at this station Q-AMS registered volcanic sulphate and Icelandic dust
62 plumes in air advected over the North East Atlantic Ocean. Concurrent observations of aerosol
63 size evolution and impact on light scattering are also discussed.

64

65 **2. Experimental**

66 A four-week field campaign was conducted in June 2007 at Mace Head Research Station, Ireland
67 ($53^{\circ}19' \text{ N}$, $9^{\circ} 54' \text{ W}$). The site has been described in detail by Jennings et al. (2003) and
68 O'Connor et al. (2008). It is located on a peninsula and the wind direction sector between 190°
69 and 300° is from the open North Atlantic Ocean providing excellent conditions for carrying out
70 marine aerosol measurements.

71 All aerosol instruments were placed in the shore laboratory about 100 m from the coastline and 5
72 m above mean sea level, MSL. They were connected to the laminar flow community air

73 sampling system, which is constructed from a 100 mm diameter stainless-steel pipe with the
74 main inlet at 10 m above ground level.

75 The size resolved non-refractory chemical composition of submicron aerosol particles was
76 measured with an Aerodyne Quadrupole Aerosol Mass Spectrometer (Q-AMS, Aerodyne,
77 Billerica, MA). The instrument is described by Jayne et al. (2000). Ionization efficiency was
78 calibrated twice (at the very beginning and the end of the campaign) by 300 nm dry ammonium
79 nitrate particles, according to the method described by Jimenez et al. (2003) and Allan et al.
80 (2003). Measurements were performed with a time resolution of 5 min, with a vaporizer
81 temperature of about 600 °C. A collection efficiency of $CE = 0.5$ was applied for the
82 measurement period discussed here. According to laboratory experiments (Matthew et al., 2008,
83 Middlebrook and Bahreini, 2008) the AMS collection efficiency depends on the particle
84 chemical composition and relative humidity of the environment. They showed that at relative
85 humidity about 80% and neutralization of sulphate particles about 50-60 %, which was the case
86 during the analysed event, collection efficiency of AMS is about 0.5.

87 The total aerosol scattering coefficient and the hemispheric backscattering coefficient were
88 measured with a TSI (TSI Incorporated, Shoreview, MN) Model 3563 three-wavelength (450;
89 550; 700 nm) integrating nephelometer.

90 Aerosol absorption measurements were performed with the Thermo scientific (Thermo Fisher
91 Scientific Inc., Waltham, MA) multi-angle absorption photometer (MAAP) instrument, model
92 5012. This instrument calculates absorbance from particles deposited on a filter using
93 measurements of both transmittance and reflectance at two different angles.

94 Aerosol size distributions were measured by a scanning mobility particle sizer (SMPS). The
95 SMPS system is composed of a differential mobility analyzer (DMA, TSI model 3071), a

96 condensation particle counter (CPC, TSI model 3010), an aerosol neutralizer (TSI 3077), a
97 control unit, and a data logging system.

98 A volatility-hygroscopic-tandem differential mobility analyser (VHTDMA) was employed to
99 simultaneously measure the volatile and hygroscopic properties of particles ranging from 10 nm
100 to 110 nm in (mobility) diameter (Johnson et al., 2004). Comparison of VHTDMA signatures
101 measured in the field with those of laboratory aerosols of known chemical composition were
102 used to infer the composition of the atmospheric particles and their mixing state. A thorough
103 description of the VHTDMA and its operating procedures has been provided by Fletcher et al.
104 (2007).

105 Radon (^{222}Rn) and lead (^{212}Pb) isotope concentrations were determined using the active deposit
106 method. The absolute error is estimated to be in the order of 20% (Polian et al., 1986; Biraud et
107 al., 2000).

108 Backward trajectories up to 96 hours were calculated, using the National Oceanic and
109 Atmospheric Administration (NOAA) hybrid single-particle lagrangian integrated trajectory
110 (HY-SPLIT) model ((Draxler and Hess, 1997). Trajectories were calculated for every hour at
111 three different altitudes: 1000, 500 and 20 meters above ground level (AGL).

112

113 **3. Results**

114 On June 26, 2007, a high pressure system over Greenland and a low situated over the North
115 Atlantic Ocean and Ireland produced a north westerly flow with 8 m/s average local wind speed
116 and quite low temperature – about 12-14 °C during the day. The relative humidity varied
117 between 80% and 90 % and particle concentration was less than 700 particles cm^{-3} , typical for
118 marine background air at Mace Head. Local wind direction shifted from 360° to 270° and
119 between 11:00 UTC and 24:00 UTC it was from the typical marine sector (which extends

120 between 190° and 300°). The air mass trajectories gradually shifted from north to west, and from
121 04:00 UTC had passed over Iceland approximately three days earlier before reaching Mace Head
122 (Fig. 1).

123

124 *3.1. Evolution of the aerosol chemical composition*

125 We observed a continuous increase in sulphate concentrations in advected air masses with
126 trajectories crossing over Iceland. Over the period of 11 hours the non-sea salt (nss)-sulphate
127 concentration increased from 1.2 to 4.6 (± 0.9) $\mu\text{g}/\text{m}^3$ (Fig. 2). Concurrent nitrate levels remained
128 low and largely unchanged indicating no major contribution from anthropogenic pollution.

129 A minor increase was observed in the level of organics, probably originating from phytoplankton
130 blooms located south-west of Iceland (NASA, 2008). However, the lack of correlation ($R^2=0.02$)
131 between organic and sulphate trends suggests that the observed increase in sulphate
132 concentration was associated with a different source. Moreover, marine biogenic nss-sulphate
133 concentrations at Mace Head station as reported by Yoon et al. (2007) are less than 0.8 $\mu\text{g}/\text{m}^3$. In
134 addition, the concurrent increase in radon concentrations (Fig. 2) supports a predominantly land
135 origin of sulphate in this air mass. Radon concentrations were initially elevated due to regional
136 contributions from Ireland but then decreased when trajectories shifted from north to north-west.
137 Later (from 12:00 UTC) it started increasing again in conjunction with air mass passage over
138 Iceland. The radon temporal trend followed the sulphate trend. Generally, the radon
139 concentration on June 26 was lower than 400 mBq/m^3 indicating an oceanic air mass (Messenger
140 et al., 2008) and little to no contact with land over the past 2-3 days. This is consistent with the
141 measurements of ^{212}Pb as lead concentration decreased after 12:00 UTC and stayed at low level
142 until the end of the day. ^{222}Rn and ^{212}Pb are both emitted by soils and can be used as continental
143 tracers. However, they have different radioactive decay time: 3.8 days for ^{222}Rn and 10.6 hours

144 for ^{212}Pb . Therefore, a decrease in concentration of the latter tracer showed the absence of a
145 recent contact with land, whereas increase in the radon concentration indicated a remote land
146 influence.

147 From these results we assume that the observed increase in sulphate concentration ($3.4 \mu\text{g}/\text{m}^3$
148 above background level) was entirely caused by advection of volcanic sulphur emissions from
149 Iceland. Using the time period of 11 hours and the $3.4 \mu\text{g}/\text{m}^3$ increase in nss-sulphate levels we
150 estimated the total sulphur flux from Icelandic volcanoes assuming that all SO_2 had been
151 converted to sulphate. The measured increase in concentration was multiplied by the total
152 volume of the plume which could be derived using the FLEXPART model (Stohl et al., 2005).
153 The mixed layer height was assumed to be 1 km. We calculated a sulphur flux of 820 t S/d.
154 Assuming constant emissions this result was scaled to the yearly sulphur flux to compare it with
155 previous estimates of annual fluxes of sulphur from Icelandic volcanoes and from
156 dimethylsulphide (DMS) emissions from the North Atlantic.

157

158 *3.2. Volcanic aerosol acidity*

159 The sulphate particles were only partially neutralized by ammonium based on the results
160 obtained by both the Q-AMS and the Volatility Hygroscopic Tandem Differential Mobility
161 Analyzer (VHTDMA). Q-AMS measured at least 35% of the total sulphate mass being a pure
162 sulphuric acid (Fig. 3) while according to VHTDMA, H_2SO_4 constituted about 26% of total
163 sulphate volume in 50nm particles.

164 The modified marine air flow touching the west coast of Ireland (Fig. 1a) in conjunction with
165 northerly wind direction brought nearly neutralized sulphate particles in the form of ammonium
166 sulphate and bisulphate (00:00 UTC - 01:00 UTC, Fig. 3). However, with trajectories shifting to
167 the west and air masses coming from the marine sector (Fig. 1b, c), the degree of neutralization

168 decreased and sulphuric acid constituted about 50 % of the total sulphate mass (10:00 UTC-
169 23:00 UTC, Fig.3).

170 Figure 4 displays a VHTDMA scan of 50 nm particles completed between 13:55 UTC and 15:26
171 UTC on June 26. The volatility curve (particle volume fraction remaining (V/V₀) against
172 thermo denuder temperature) had 2 distinct volatilisation steps. The first component evaporated
173 at 80-140°C and the second component evaporated at 160-220°C. Comparison with a VHTDMA
174 scan of laboratory generated, partially neutralised sulphuric acid (H₂SO₄) particles (Johnson et al.
175 2005) suggests that the more volatile component is H₂SO₄ and the less volatile component is
176 partially neutralised H₂SO₄ (ammoniated sulphate). For the ambient scan the volume fraction of
177 H₂SO₄ is 26%. A repeat scan conducted between 16:15 UTC and 16:53 UTC was very similar to
178 the original scan. The volume fraction of H₂SO₄ was, again, 26%.

179 The degree of neutralisation was calculated assuming that any ammoniated sulphate existed as
180 letovicite ((NH₄)₃H(SO₄)₂). This assumption is based on the measured fraction of sulphuric acid
181 and the H₂O-(NH₄)₂SO₄-H₂SO₄ phase diagram presented by Tang et al. (1978). The per-particle
182 volumes of H₂SO₄ and (NH₄)₃H(SO₄)₂ were calculated from the initial particle diameters and
183 particle diameters at 150°C and 220°C. These volumes were converted to mole numbers using
184 density and molecular weight. The density of H₂SO₄ was calculated according to the
185 parameterisation of Tang (1996). Finally, considering the stoichiometry of letovicite the
186 ammonium to sulphate ratio was calculated to be 110.5%.

187 However, with respect to particle size the Q-AMS covered the 40-1000 nm diameter range of
188 particles, whereas VHTDMA measured the composition of only 50 nm particles at that time.
189 Therefore the combined results suggest that there was a greater degree of neutralisation for
190 smaller particles. Previous studies e.g., by Fletcher et al. (2007) at Cape Grim station and
191 Tomlinson et al. (2007) over the south-eastern Pacific also reported a relatively stronger

192 neutralization in lower particle sizes. They suggested that size dependent acidity could be
193 explained by H₂SO₄ being added to the aerosol by in-cloud aqueous phase processes faster than
194 it can be neutralized by the limited available ammonium. On the other hand, smaller particles
195 may simply be neutralized by the limited ammonium more readily due to their higher surface-
196 volume ratio (McMurry et al. 1983). In our study both instruments showed the presence of pure
197 sulphuric acid in the particles which is consistent with previous study of Satsumabayashi et al.
198 (2004) who showed that aerosols affected by volcanic emissions were strongly acidic as the
199 excess amount of SO₄²⁻ exhausted ammonium and partially expelled NO₃⁻ and Cl⁻. Furthermore,
200 Stothers and Rampino (1983) demonstrated that the largest acidity signals in old Greenland ice
201 are due to European (Mediterranean and Icelandic) volcanic eruptions. Typically, the ammonium
202 to sulphate ratio measured near a volcanic source is much lower compared to a site further
203 downwind (Johnson and Parnell, 1986; Mather et al., 2003).

204

205 *3.3. Aerosol radiative absorption and scattering*

206 In addition to sulphate plume, an increase in absorption was registered by multi-angle absorption
207 photometer (MAAP). Figure 6 shows that noticeable amount of absorbing material was
208 measured between 16:15 UTC and 20:30 UTC. The Moderate Resolution Imaging
209 Spectroradiometer (MODIS) flying on NASA's Terra satellite captured the image of dust plumes
210 blowing off the southern coast of Iceland over the North Atlantic Ocean on June 23, 2007 (Fig.
211 5). Thus following this event, elevated concentrations of light absorbing particles were
212 encountered at Mace Head (Fig. 6). MAAP is a filter-based technique for measuring aerosol light
213 absorption, it rely on the change in transmission of light through a filter as it is loaded with
214 aerosol to determine the aerosol absorption coefficient. Similar to other filter-based techniques
215 measurements can be biased during specific conditions (Lack et al., 2008) such as high loadings

216 of dust aerosol. Dust particles can both absorb and scatter sunlight (Miller et al., 2004).
217 Consistent with these properties our measurements showed a good correlation between light
218 absorption and both back and total (back plus forward) scattering coefficients (Fig. 6). Several
219 previous studies demonstrated that dust events increased scattering coefficients and
220 nephelometer could be used as a good indicator of dust particle advection (Ichoku C. et al. 1999;
221 Kim et al., 2004; Derimian et al., 2006). During advection of Icelandic dust to Mace Head , the
222 total scattering coefficient followed similar trends at all three wavelengths (450, 550, 700 nm)
223 whereas the backscattering coefficient was more spread between different wavelengths of light
224 although they showed a similar time trend. These differences between wavelengths became
225 significant (~15-20%) when the fraction of the organic aerosol material increased (12:00-13:00
226 UTC, 20:00-21:00 UTC) showing an inhomogeneous particle size distribution. In addition,
227 Figure 6 shows that the light-scattering associated by sulphate aerosol was lower compared to
228 the dust particles. Aerosol light scattering coefficients peaked at the same time as absorption
229 maximum and only qualitatively followed sulphate concentration increase.

230

231 *3.4. Aerosol size distribution*

232 During the studied event, the aerosol size distribution was bimodal with well defined Aitken and
233 accumulation modes. Figure 7 presents the temporal evolution of the aerosol size spectrum.
234 Initially, a higher fraction of sulphate resulted in the growth of both accumulation and Aitken
235 mode particles. However, this changed later due to the increasing fraction of dust particles.
236 Consequently from 16:30 UTC we observed both higher absorption levels and a concurrent
237 change in the size distribution (17:30 UTC). The Aitken mode diameter continued to increase
238 while the accumulation mode diameter shifted towards smaller sizes (Table 1). In addition, dust
239 particles increased the number concentration in both the Aitken and accumulation modes.

240 From 20:30 UTC air masses were advected from the North Atlantic Ocean which had not passed
241 over Iceland. In this context, a rapid decrease in sulphate concentrations and significant change
242 in the aerosol size spectrum was observed resulting in typical aerosol size distribution for a very
243 clean air mass at Mace Head (Yoon et al., 2007).

244

245 **4. Discussions**

246 In general, the climate relevant implications of volcanic eruptions have been recognized in
247 previous studies (Toon and Pollack, 1980; Gilliland, 1982; Rampino and Self, 1984; Minnis et
248 al., 1993; Robock A., 2000). However, quasi-continuous non-eruptive emissions may have an
249 even stronger incremental climatic impact than the relatively brief cataclysmic eruptions (Graf et
250 al., 1997). For example, the annual sulphur input into the atmosphere from Icelandic volcanoes is
251 of the same range as the total sulphur flux from the dimethylsulphide over the whole North
252 Atlantic Ocean, 0.5 TgS/yr (Halmer et al., 2002) and 1.3 TgS/yr (Kettle and Andreae, 2000)
253 respectively. Moreover, we estimated that Icelandic volcanogenic sulphur flux was about 0.3
254 TgS/yr (see previous section for details) suggesting that a large amount of sulphur emissions
255 from Icelandic volcanoes can reach distances larger than 1000 km (Iceland to Ireland distance is
256 approximately 1300 km). Such calculations, based on one event, should be considered as a rough
257 estimate of the regional impact of degassing sulphur emissions; however it corresponds well with
258 the previous calculations of total sulphur flux from Icelandic volcanoes (Halmer et al., 2002).
259 Thus despite its relative point source character the distribution of sulphur from Icelandic
260 volcanoes over the North Atlantic region was comparable to the larger scale input from marine
261 biogenic sources.

262 The most obvious and well known volcanic effect is on solar radiation, since the sulphate
263 particles are about the same size as the visible light wavelength (Robock, 2000). Though only a

264 relatively small fraction of sulphate is directly emitted from volcanoes, the bulk of the sulphate
265 aerosol is formed during the long range transport of the emissions by both gas and aqueous phase
266 oxidation of SO₂ (Hegg, 1985), affecting the resulting aerosol size distribution. Our observations
267 of a typical aerosol bimodal size distribution during the volcanic plume event suggest a
268 significant cloud processing of the aerosol along the trajectory path where accumulation mode
269 was formed by cloud activation of Aitken mode particles (Hoppel et al., 1986; Fitzgerald, 1991;
270 Bott, 1999; O'Dowd et al., 2000).

271 Presumably two processes took place during this transport: a new sulphate aerosol formation
272 and its subsequent neutralization by cations such as ammonium. As measurements near
273 volcanoes show highly acidic aerosol (Johnson and Parnell, 1986; Mather et al., 2003;
274 Satsumabayashi et al., 2004), the partially neutralised aerosol measured at Mace Head indicates
275 the chemical aerosol evolution during air mass transport. Along with the chemical transformation
276 the physical aerosol properties have been changing as well, with the increasing fraction of
277 sulphate resulting in the growth of both accumulation and Aitken mode particles. Moreover,
278 concurrent advection of dust particles from Icelandic deserts contributed to further modifications
279 of the aerosol properties. Dust particles were identified by two independent albeit indirect
280 measurements using the three-wavelength integrating nephelometer and the multi-angle
281 absorption photometer. We observed a corresponding increase by about 60% in light absorption
282 and scattering caused by advected sulphate and dust particles which indicates their strong
283 climatic implications.

284

285 **5. Conclusions**

286 Advection of volcanogenic sulphate aerosol from Iceland significantly increased sulphate
287 concentrations at Mace Head. Moreover it was shown that the corresponding volcanic plume

288 caused a substantial modification in the aerosol chemical composition and size distribution over
289 the North Atlantic region during transport. Over the period of 11 hours the non-sea salt sulphate
290 concentration increased by a factor of four while concurrent nitrate and organic levels remained
291 low and largely unchanged. The sulphate particles were only partially neutralized. The Q-AMS
292 measurements showed that at least 35% of the total sulphate mass was pure sulphuric acid in
293 submicrometer (PM1) aerosol. Concurrent VHTDMA measurements showed that H₂SO₄
294 constituted about 26% of the total sulphate volume in particles of 50 nm diameter size. The
295 combined results suggest that there was a relatively larger degree of neutralisation by ammonium
296 in smaller particles. The predominant fraction of sulphate aerosol is assumed to have been
297 formed by aqueous phase oxidation of SO₂ based on the efficiency of this process and the cloud
298 cover associated with the air mass trajectories. A concurrent dust outbreak from Iceland
299 increased the levels of absorbing material and the light-scattering. Aerosol light scattering
300 coefficients peaked at the same time as absorption maximum and qualitatively followed sulphate
301 concentration increase. Evaluated sulphur flux demonstrated that a large amount of the total
302 (non-eruptive) sulphur emissions from Icelandic volcanoes can reach distances larger than 1000
303 km. These results in conjunction with previous research suggest that volcanogenic emissions and
304 Aeolian dust from Arctic deserts in Iceland can be potentially significant regional sources of
305 aerosols over the North Atlantic and therefore should be adequately considered in regional and
306 global climate models.

307

308 **Acknowledgments**

309 This work was supported by the EU projects ACCENT (subproject Access to research
310 infrastructures), EUSAAR TNA, SFI (Science Foundation Ireland, grant 08/RFP/GEO1233),

311 EPA Ireland and ESF (European Science Foundation, activity: INTROP). Authors wish to thank
312 anonymous reviewers for their constructive and helpful comments.

313

314 **References**

315 Allan J.D., Jimenez J.L., Williams P.I., Alfarra M.R., Bower K.N., Jayne J.T., Coe H., Worsnop
316 D.R., 2003. Quantitative sampling using an Aerodyne aerosol mass spectrometer 1. Techniques
317 of data interpretation and error analysis. *Journal of Geophysical Research* 108 (D3), 4090–4100.

318 Arnalds O., Gísladóttir F. O., Sigurjónsson H., 2001. Sandy deserts of Iceland: an overview.
319 *Journal of Arid Environments* 47, 359–371

320 Berresheim H., Jaeschke W., 1983. The contribution of volcanoes to the global atmospheric
321 sulfur budget, *Journal of Geophysical Research* 88, 3732-3740.

322 Biraud S., Ciais P., Ramonet M., Simmonds P., Kazan V., Monfray P., O'Doherty S., Spain T. G.,
323 Jennings S. G., 2000. European greenhouse gas emissions estimated from continuous
324 atmospheric measurements and radon 222 at Mace Head, Ireland. *Journal of Geophysical*
325 *Research* 105(D1), 1351–1366.

326 Bott A., 1999. A numerical model of the cloud-topped planetary boundary-layer: cloud
327 processing of aerosol particles in marine stratus. *Environmental Modelling and Software* 14,
328 635-643.

329 Charlson R. J., Lovelock J. E., Andreae M. O., Warren S. G., 1987. Oceanic phytoplankton,
330 atmospheric sulphur, cloud albedo and climate. *Nature* 326, 655–661.

331 Derimian Y., Karnieli A., Kaufman Y. J., Andreae M. O., Andreae T. W., O. Dubovik, W.
332 Maenhaut, I. Koren, and B. N. Holben, 2006. Dust and pollution aerosols over the Negev desert,
333 Israel: Properties, transport, and radiative effect, *Journal of Geophysical Research* 111, D05205,
334 doi:10.1029/2005JD006549.

335 Draxler R.R., Hess G.D., 1997. Description of the Hysplit_4 modeling system. NOAA Tech
336 Memo ERL ARL-224, 24p. (<http://www.arl.noaa.gov/ready/hysplit4.html>)

337 Fitzgerald J.W., 1991. Marine aerosols: A review. *Atmospheric Environment - Part A General*
338 *Topics* 25, Issue 3-4, 533-545.

339 Fletcher C. A., Johnson G. R., Ristovski Z. D., Harvey, M., 2007. Hygroscopic and volatile
340 properties of marine aerosol observed at Cape Grim during the P2P campaign. *Environmental*
341 *Chemistry* 4, 162-171.

342 Gilliland, R. L., 1982. Solar, volcanic, and CO₂ forcing of recent climatic changes, *Climatic*
343 *Change* 4, 111–131.

344 Glasow R., Bobrowski N., Kern C., 2008. The effects of volcanic eruptions on atmospheric
345 chemistry. *Chemical Geology*, Article in Press.

346 Graf H.-F., Feichter J. , Langmann B., 1997. Volcanic sulfur emissions: Estimates of source
347 strength and its contribution to the global sulfate distribution, *Journal of Geophysical Research*
348 102(D9), 10,727–10,738.

349 Textor C., Graf H. F., Timmreck C., and Robock A., 2004. Emissions from volcanoes. In
350 *Emissions of Atmospheric Trace Compounds*, Claire Granier, Paulo Artaxo, and Claire Reeves,
351 Eds., (Kluwer, Dordrecht), 269-303.

352 Halmer M.M., Schmincke H.U., Graf H.F., 2002. The annual volcanic gas input into the
353 atmosphere, in particular into the stratosphere: a global data set for the past 100 years. *Journal of*
354 *Volcanology and Geothermal Research* 115, 511-528.

355 Hegg D.A., 1985. The importance of liquid phase oxidation of SO₂ in the troposphere. *Journal*
356 *of Geophysical Research* 90, 3773-3779.

357 Hoppel W. A., Frick G. M., Larson R. E., 1986. Effect of nonprecipitating clouds on the aerosol
358 size distribution in the marine boundary layer, *Geophysical Research Letters* 13, 125–128.

359 Ichoku C., Andreae M.O., Andreae T.W., Meixner F.X., Schebeske G., Formenti P., Maenhaut
360 W., Cafmeyer, J., Ptasinski, J., Karnieli, A., Orlovsky L., 1999. Interrelationships between
361 aerosol characteristics and light scattering during late winter in an Eastern Mediterranean arid
362 environment, *Journal of Geophysical Research* 104(D20), 24,371–24,393.

363 Jayne J.T., Leard D.C., Ahang X., Davidovits P., Smith K.A., Kolb C.E., Worsnop D.R., 2000.
364 Development of an aerosol mass spectrometer for size and composition analysis of submicron
365 particles. *Aerosol Science and Technology* 33 (1–2), 49–70.

366 Jennings S. G., Kleefeld C., O’Dowd, Junker C., Spain T. G., O’Brien P., Roddy A. F.,
367 O’Connor T. C., 2003. Mace Head atmospheric research station—Characterization of aerosol
368 radiative parameters. *Boreal Environment Research* 8, 303 – 314.

369 Jimenez J.L., Jayne J.T., Shi Q., Kolb C.E., Worsnop D.R., Yourshaw I., Seinfeld J.H., Flagan
370 R.C., Zhang X., Smith K.A., Morris J.W., Davidovits P., 2003. Ambient aerosol sampling using
371 the Aerodyne Aerosol Mass Spectrometer. *Journal of Geophysical Research* 108 (D7), 8245–
372 8258.

373 Johnson N. and Parnell R. A., 1986. Composition, distribution and neutralization of ‘acid rain’
374 derived from Masaya volcano, Nicaragua. *Tellus* 38B, 106–117.

375 Johnson G. R., Ristovski Z., Morawska L., 2004. Method for measuring the hygroscopic
376 behaviour of lower volatility fractions in an internally mixed aerosol. *Journal of Aerosol Science*
377 35, 443–455.

378 Johnson G. R., Ristovski Z. D., D’Anna B., Morawska L., 2005. Hygroscopic behaviour of
379 partially volatilised coastal marine aerosols using the volatilisation and humidification tandem
380 differential mobility analyser technique. *Journal of Geophysical Research* 110, D20203.

381 Kettle A. J., Andreae M. O., 2000. Flux of dimethylsulfide from the oceans: A comparison of
382 updated data sets and flux models, *Journal of Geophysical Research* 105, 26,793–26,808.

383 Kim K. W., He Z., Kim Y. J., 2004. Physicochemical characteristics and radiative properties of
384 Asian dust particles observed at Kwangju, Korea, during the 2001 ACE-Asia intensive
385 observation period, *Journal of Geophysical Research* 109, D19S02, doi:10.1029/2003JD003693.

386 Lack D., Cappa C., Covert D., Baynard T., Massoli P., Sierau B., Bates T., Quinn P., Lovejoy E.,
387 Ravishankara A. R. Bias in Filter-Based Aerosol Light Absorption Measurements Due to
388 Organic Aerosol Loading: Evidence from Ambient Measurements (2008) *Aerosol Science and*
389 *Technology*, 42:1033–1041.

390 Mather T. A., Allen A. G., Oppenheimer C., Pyle D. M., McGonigle A. J. S., 2003. Size-
391 Resolved Characterisation of Soluble Ions in the Particles in the Tropospheric Plume of Masaya
392 Volcano, Nicaragua: Origins and Plume Processing. *Journal of Atmospheric Chemistry* 46, 207–
393 237.

394 Matthew B.M., Middlebrook A.M., Onasch T.B., 2008. Collection Efficiencies in an Aerodyne
395 Aerosol Mass Spectrometer as a Function of Particle Phase for Laboratory Generated Aerosols.
396 *Aerosol Science and Technology* 42(11), 884-898, DOI: 10.1080/02786820802356797

397 McMurry P. H., Takano H., Anderson G. R., 1983. Study of the Ammonia (Gas)- Sulphuric Acid
398 (Aerosol) Reaction Rate. *Environmental Science and Technology* 17, 347-352.

399 Messenger C., Schmidt M., Ramonet M., Bousquet P., Simmonds P., Manning A., Kazan V.,
400 Spain G., Jennings S. G., Ciais P., 2008. Ten years of CO₂, CH₄, CO and N₂O fluxes over
401 Western Europe inferred from atmospheric measurements at Mace Head, Ireland. *Atmospheric*
402 *Chemistry and Physics Discussions* 8, 1191–1237.

403 Middlebrook A. Bahreini R., 2008. Applying Laboratory Collection Efficiencies to Ambient
404 Field Data. AMS Users' Meeting 2008. Accessed on 18.02.2009
405 http://cires.colorado.edu/jimenez-group/UsrMtg9/09_Middlebrook_CE.pdf

406 Miller R.L., Tegen I., Perlwitz J., 2004. Surface radiative forcing by soil dust aerosols and the
407 hydrologic cycle. *Journal of Geophysical Research* 109 (D4), D04203.

408 Minnis, P., E. F. Harrison, L. L. Stowe, G. G. Gison, F. M. Denn, D. R. Doelling, and W. L.
409 Smith Jr., 1993. Radiative climate forcing by the Mount Pinatubo eruption, *Science* 259, 1411–
410 1415.

411 NASA (2008). Accessed on 11/05/2009.
412 <http://earthobservatory.nasa.gov/NaturalHazards/view.php?id=18595&oldid=14345>.

413 O'Connor T.C., Jennings S.G., O'Dowd C.D., 2008. Highlights of fifty years of atmospheric
414 aerosol research at Mace Head, *Atmospheric Research* 90, 338-355.

415 O'Dowd C.D., Smith M.H., 1993./ Physicochemical properties of aerosols over the northeast
416 Atlantic: evidence for wind-speed-related submicron sea-salt aerosol production. *Journal of*
417 *Geophysical Research* 98 (D1), 1137-1149.

418 O'Dowd C. D., Low, J. A., Smith M. H., 2000. The effect of clouds on aerosol growth in the
419 rural atmosphere. *Atmospheric Research* 54, 4, 201-221.

420 Polian G., Lambert G., Ardouin B., and Jegou A., 1986. Long-range transport of continental
421 radon in subantarctic and antarctic areas, *Tellus* 38B, 178–189.

422 Prospero J. M., Arnalds Ó., Olafsson H., Bullard J. E., Hodgkins R., 2008. Iceland Dust Storms
423 Linked to Glacial Outwash Deposits and to Sub-Glacial Flood (Jökulhlaup) Events, *Eos Trans.*
424 *AGU* 89 (53), Fall Meeting Supplementary, Abstract A13E-08

425 Rampino, M. R., and S. Self, 1984. Sulphur-rich volcanic eruptions and stratospheric aerosols,
426 *Nature*, 310, 677–679.

427 Robock A., 2000. Volcanic eruptions and climate. *Reviews of Geophysics* 38, 191–219.

428 Satsumabayashi H., Kawamura M., Katsuno T., Futaki K., Murano K., Carmichael G. R., Kajino
429 M., Horiguchi M., Ueda H., 2004. Effects of Miyake volcanic effluents on airborne particles and
430 precipitation in central Japan, *Journal of Geophysical Research* 109, D19202.

431 Savoie D. L., Arimoto R., Keene W. C., Prospero J. M., Duce R. A., Galloway J. N., 2002.
432 Marine biogenic and anthropogenic contributions to non-sea-salt sulfate in the marine boundary
433 layer over the North Atlantic Ocean, *Journal of Geophysical Research* 107(D18), 4356

434 Stohl A., Forster C., Frank A., Seibert P. and Wotawa G., 2005. Technical Note: The Lagrangian
435 particle dispersion model FLEXPART version 6.2. *Atmospheric Chemistry and Physics* 5, 2461-
436 2474. http://niflheim.nilu.no/~burkhart/EUCAARI/MHD/MHD_200706/

437 Stothers r. B., Rampino M. R., 1983. Historic Volcanism, European Dry Fogs, and Greenland
438 Acid Precipitation, 1500 B.C. to A.D. 1500. *Science, New Series*, Vol. 222, 4622, 411-413.

439 Tang I. N., Munkelwitz H. R., Davis J. G., 1978. Aerosol Growth Studies- IV. Phase
440 Transformation of Mixed Salt Aerosols in a Moist Atmosphere. *Journal of Aerosol Science* 9,
441 505-511.

442 Tang I. N., 1996. Chemical and size effects of hygroscopic aerosols on light scattering
443 coefficients. *Journal of Geophysical Research* 101, 19,245–19,250.

444 Tomlinson J. M., Li R., Collins D. R., 2007. Physical and chemical properties of the aerosol
445 within the southeastern Pacific marine boundary layer. *Journal of Geophysical Research* 112,
446 D12211, doi:10.1029/2006JD007771.

447 Toon, O. B., and Pollack J. B., 1980. Atmospheric aerosols and climate, *American Scientist* 68,
448 268–278.

449 Yoon Y. J., Ceburnis D., Cavalli F., Jourdan O., Putaud J. P., Facchini M. C., Decesari S., Fuzzi
450 S., Jennings S. G., O’Dowd C. D., 2007. Seasonal characteristics of the physico-chemical

451 properties of North Atlantic marine atmospheric aerosols. *Journal of Geophysical Research* 112,
452 D04206; doi: 10.1029/2005JD007044.

Table1[Click here to download Table: Table 1.doc](#)

Time, UTC	11:30	14:00	15:50	17:30	19:00	20:00	21:30
Aitken mode median diameter, nm	34 ±0.1	34 ±0.1	35 ±0.1	41 ±0.2	46 ±0.3	52 ±0.3	36 ±0.2
Number concentration, 1/cm ³	613±11	471±9	439±9	383±7	473±8	437±9	218±3
Accumulation mode median diameter, nm	162 ±4	184 ±3	191 ±4	186 ±2	163 ±4	154 ±2	209 ±4
Number concentration, 1/cm ³	130±1	127±2	129±2	158±2	209±2	263±4	108±1

Fig. 1. Evolution of air mass back trajectories, calculated for June 26, 2007 (NOAA HYSPLIT): a) 02:00 UTC; b) 11:00 UTC; c) 19:00 UTC. Backward trajectories length was up to 96 hours at three different altitudes: 1000, 500 and 20 meters above ground level.

Fig. 2. Temporal trends of chemical composition of PM1 aerosol, measured by Q-AMS and concurrent radon concentrations on June 26, 2007.

Fig. 3. Time trends of ammonium to sulphate molar ratios in PM1 aerosol, measured by Q-AMS on June 26, 2007. There are 2 moles of ammonium for every mole of sulphate consequently when sulphate is fully neutralized in the form of ammonium sulphate the ratio is 200%, when sulphate is ammonium bisulphate ratio is 100%, and for particulate sulphuric acid ratio is 0.

Fig. 4. VHTDMA scan of 50 nm particles completed between 13:55 UTC and 15:26 UTC on June 26. Volume fraction remaining (V/V_0) and Hygroscopic Growth Factor (HGF) at 90% RH are both displayed as a function of thermo denuder temperature. Also plotted are the corresponding curves for 100nm partially neutralised H_2SO_4 particles measured in the laboratory by Johnson et al. (2005). The two steps in the laboratory measured volatility curve correspond to evaporation of H_2SO_4 (60-150°C) and ammoniated sulphate (160-220°C).

Fig. 5. Dust storm blowing off the southern coast of Iceland over the North Atlantic Ocean on June 23, 2007 (NASA, 2008).

Fig. 6. Enhancement of scattering coefficients and absorption due to increase in sulphate concentration and dust particles levels on June 26, 2007.

Fig. 7. Evolution of bimodal size distribution, measured by SMPS on June 26, 2007.

Table 1. Summary of the modal parameters obtained by fitting lognormal functions to aerosol number size distribution measured by SMPS in Mace Head on June 26.

Figure 1

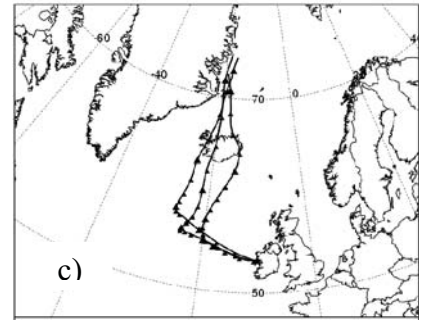
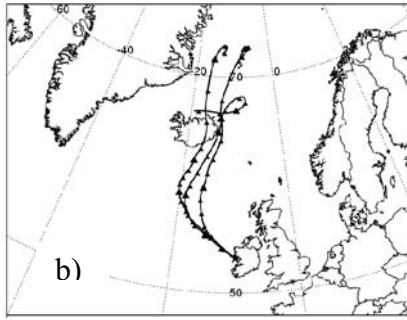
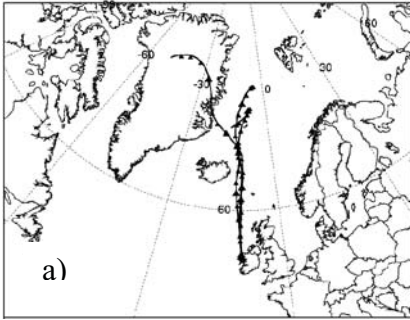


Figure2

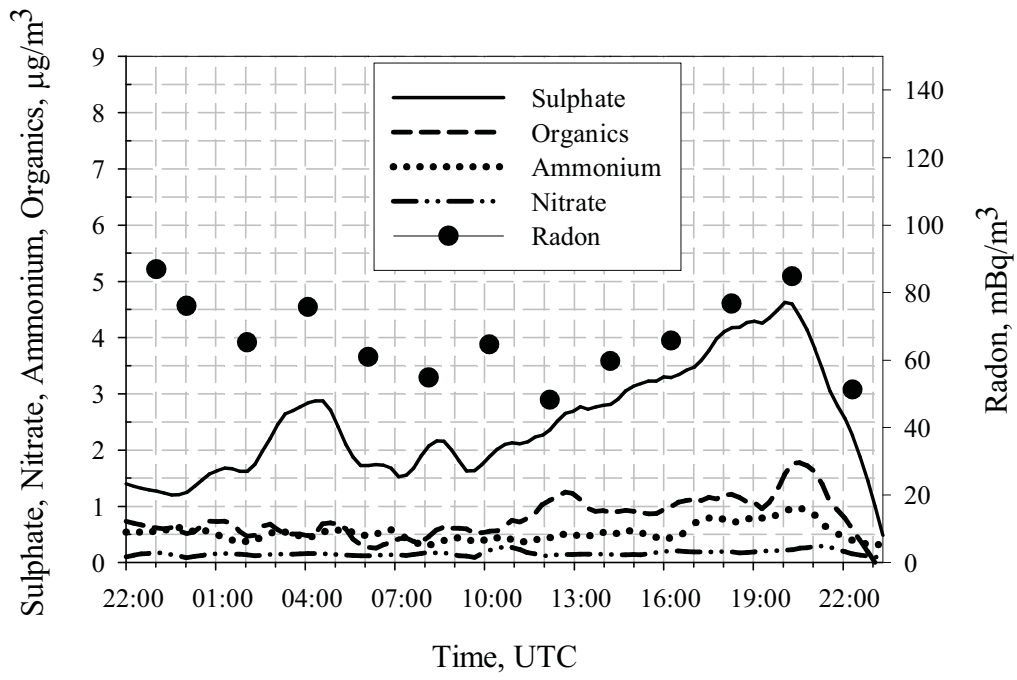


Figure 3

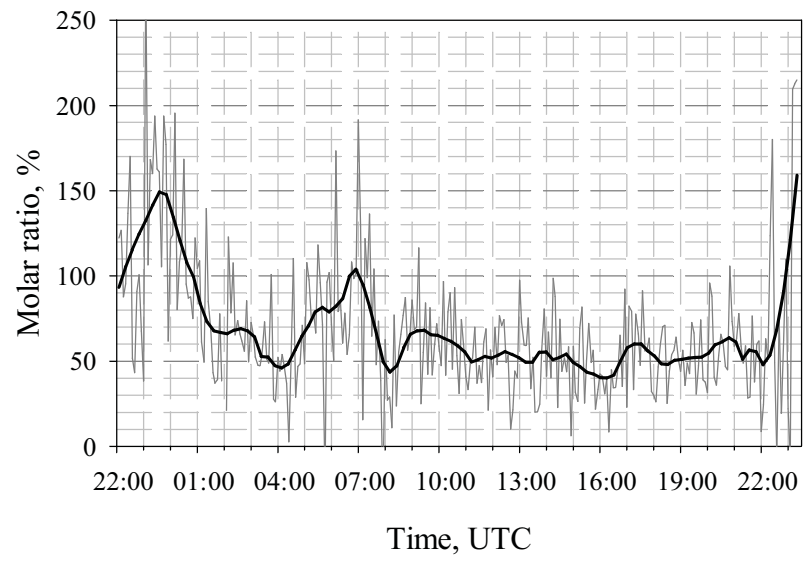


Figure 4

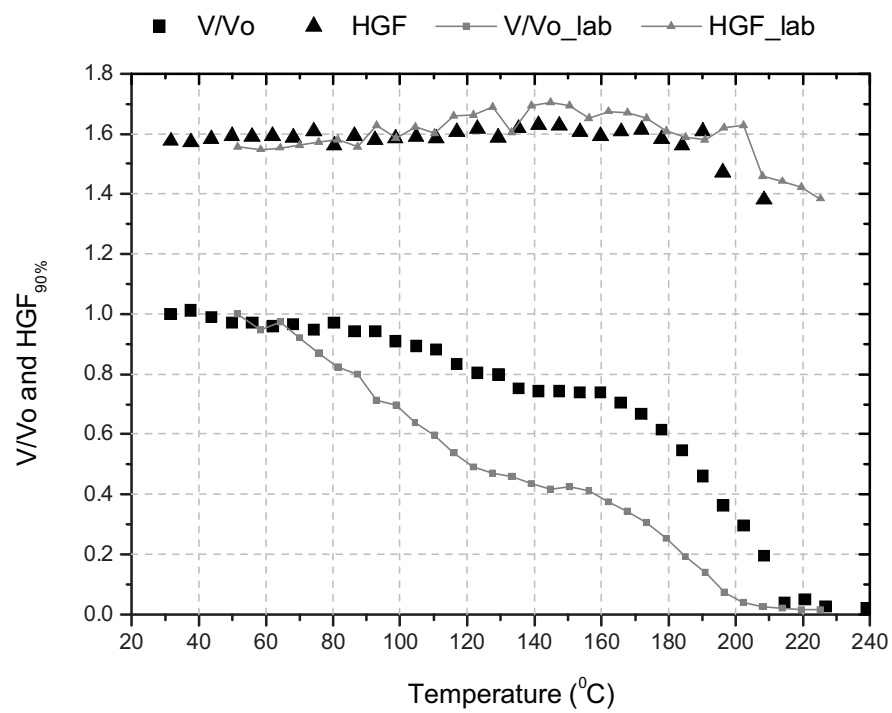


Figure 5
[Click here to download high resolution image](#)

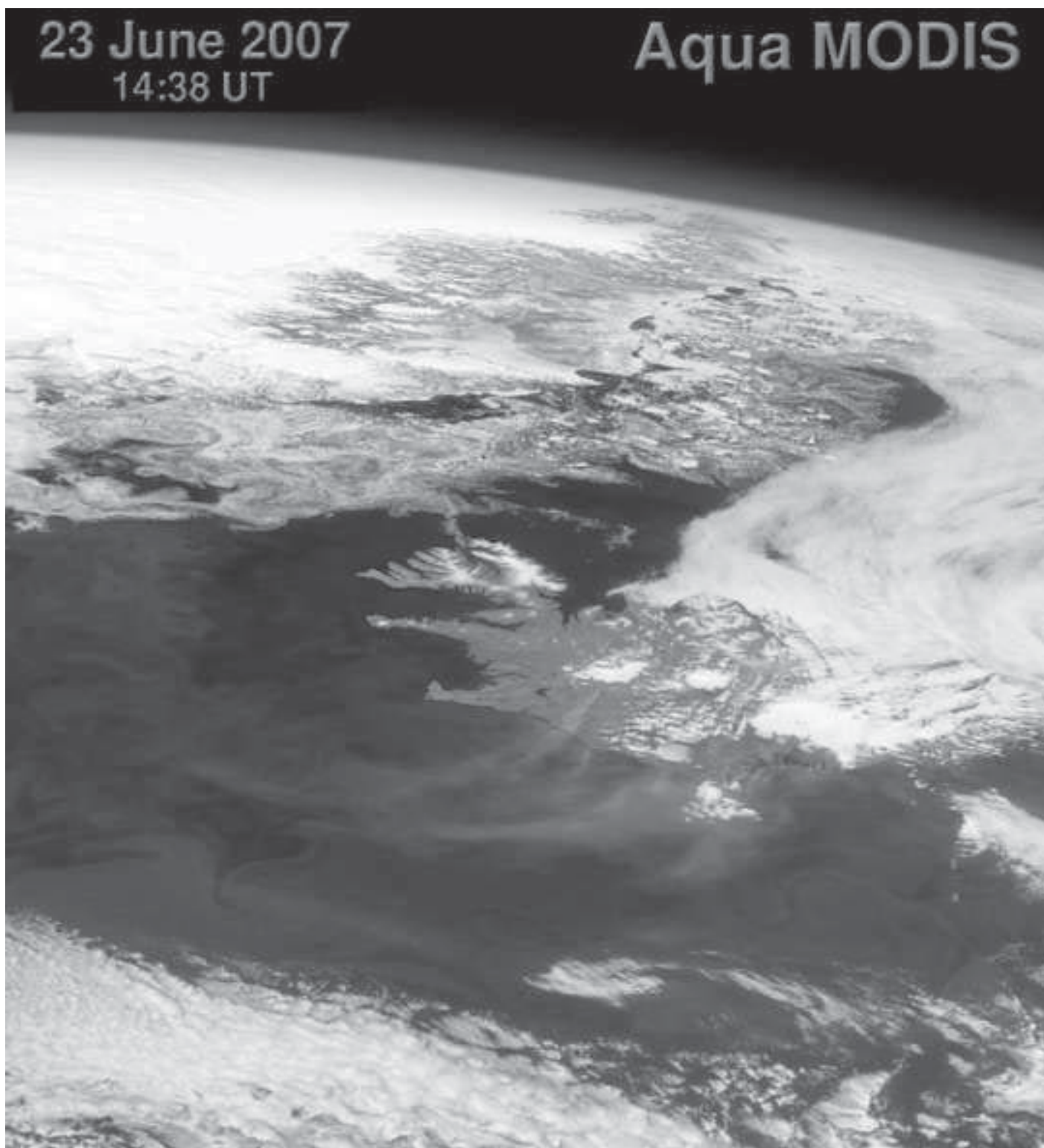


Figure 5 colour for the Web
[Click here to download high resolution image](#)

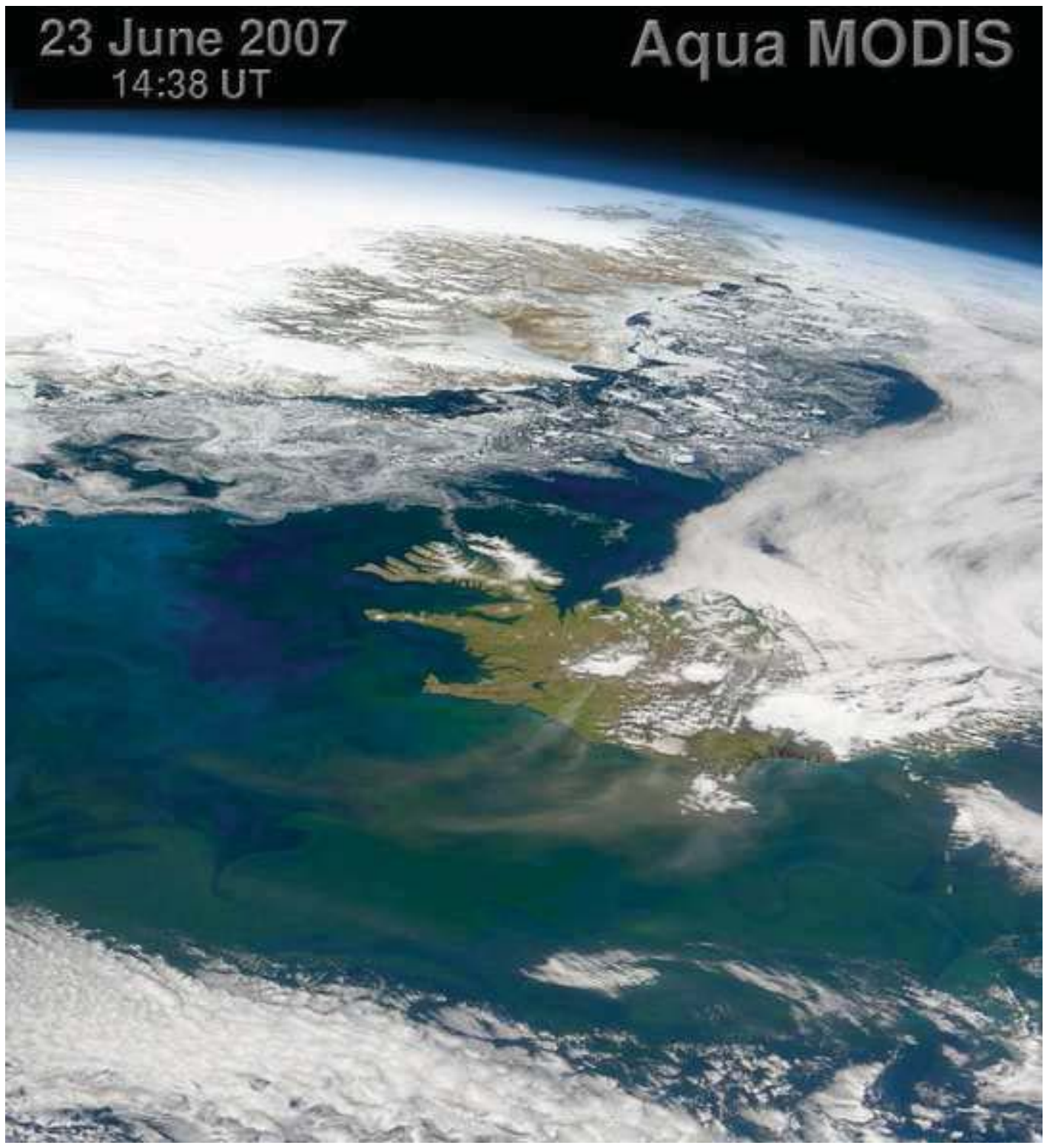


Figure6

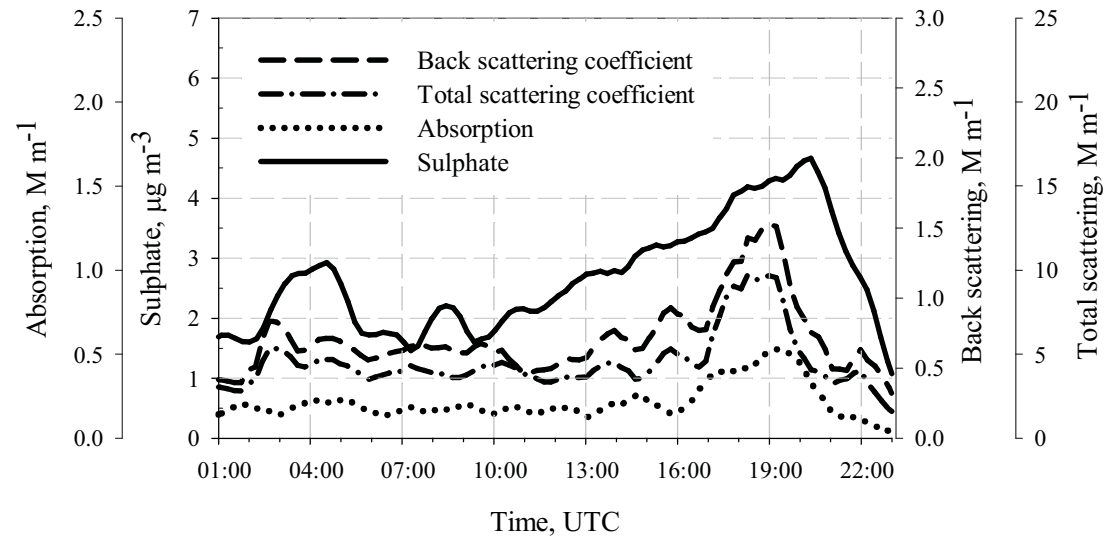


Figure 7

